SENSITIVITY OF SINGLE DIODE MODELS FOR PHOTOVOLTAIC MODULES TO METHOD USED FOR PARAMETER ESTIMATION

Clifford W. Hansen[1a], Amanda Luketa-Hanlin[2], Joshua S. Stein[1b]

1a. (Corresponding Author) Sandia National Laboratories, P.O. Box 5800 MS 1033, Albuquerque, NM 87185-1033 USA. tel: (505)-284-1643, fax: (505)-844-2890, email: cwhanse@sandia.gov

1b. tel: (505) 845-0936, email jsstein@sandia.gov

2. University of Colorado, 1111 Engineering Drive, UCB 427, Boulder, CO 80309-0427, USA. Email: amlu8066@colorado.edu

ABSTRACT: Parameter estimation for the single diode equivalent circuit model is challenging due to the implicit transcendental relationship between current and voltage. Various methods for parameter estimation have been proposed. We compare the performance of the single diode model for several photovoltaic modules with model parameters determined by applying different methods to a set of IV curves measured outdoors for each module. We found that a recently-developed sequential estimation method produced calibrated models more reliably, and with less error, than obtained when using the other estimation techniques we considered. We found that the single diode equation can be adequately fit to each of a set of IV curves measured over a wide range of conditions. However, the additional equations, which describe how model parameters change with temperature and irradiance, are the source of systematic model errors. The sequential estimation method can enable discovery of more appropriate model equations. We confirmed our findings through analysis of six PV modules representative of a variety of technologies.
Keywords: Modeling, Parameter estimation, Single diode model, Calibration.

1 INTRODUCTION

A single diode equivalent circuit model is a popular way to represent the electrical performance of a photovoltaic (PV) module. A single diode model is formulated by extending the ideal diode law to account for parasitic series and shunt resistances [1] and by adding equations that describe how model terms (e.g., photocurrent) vary with irradiance and cell temperature. Various single diode models exist (e.g., [2], [3]), and some implementations are in wide commercial use (e.g., [4]).

The primary challenge to the use of a single diode model is the determination of values for its parameters. Many parameter estimation techniques have been proposed (see Sect. 3 for a brief overview) but no standard method has been adopted by the broad community. Without a standard method for estimating model parameters, different modelers may obtain different model parameter values even when the parameter values are derived from a common set of measurements. Uncertainty regarding model parameters contributes to the uncertainty that is ascribed to predictions of PV system performance. Consequently, to reduce uncertainty about system performance predictions, it is necessary to understand how model results are affected by the method chosen to estimate the model's parameters. Careful analysis of these effects may lead to model improvement, and perhaps a consensus regarding standard methods for parameter estimation.

We analyze the performance of a single diode equivalent circuit model [3] for several PV modules using parameters obtained by three different estimation methods. We first outline the single diode model that serves to illustrate our proposed method (Sect. 2). We review parameter estimation methods in Sect. 3, describe the methods we employed, and describe the modules considered. Finally, we analyze the resulting parameters and the errors in the performance predictions for the modules (Sect. 4).

2 SINGLE DIODE MODELS

The single diode model for a solar cell (e.g., [3], Eq. 1) can be derived from physical principles (e.g., [1]) and is often interpreted by an equivalent circuit comprising a current source, a diode, a parallel resistor and a series resistor. For a module comprising N_S identical cells in series, the I-V characteristic is expressed as:

$$I = I_L - I_O\left[\exp\left(\frac{V+IR_s}{nN_SV_{th}}\right)-1\right]-\frac{V+IR_s}{R_{sh}} \quad (1)$$

where n is the diode ideality factor, and $V_{th} = kT_C/q$ is the thermal voltage (V) per cell, which is determined from cell temperature T_C (K), Boltzmann's constant k (eV/K) and the elementary charge q (Coulombs). The parameters I_L, I_O, R_s, R_{sh}, and n are commonly referred as "the five parameters" from which the term "five parameter model" originates. In this presentation, values for the series resistance R_s and shunt resistance R_{sh} are considered at the module level; cell level values of these quantities can be obtained by dividing the module values by N_S (e.g., [5]).

Eq. (1) describes the single I-V curve associated with values for the parameters I_L, I_O, R_S, R_{SH}, and n. To obtain a complete model for the electrical performance of a module over all irradiance and temperature conditions, Eq. (1) is supplemented with equations that define how each of the five parameters change with irradiance and/or cell temperature; these equations often introduce additional parameters to the model. Here, we demonstrate the effects of different parameter estimation methods using the performance model described by De Soto et al. [3]:

$$I_L = I_L\left(E,T_C\right) = \frac{E}{E_0}\left[I_{L0}+\alpha_{Isc}\left(T_C-T_0\right)\right] \quad (2)$$

$$I_O = I_{O0}\left[\frac{T_C}{T_0}\right]^3\exp\left[\frac{1}{k}\left(\frac{E_g\left(T_0\right)}{T_0}-\frac{E_g\left(T_C\right)}{T_C}\right)\right] \quad (3)$$

$$E_g(T_C) = E_{g0}\left(1 - 0.0002677\left(T_C - T_0\right)\right) \quad (4)$$

$$R_{SH} = R_{SH0}\left(E_0/E\right) \quad (5)$$

where the subscript $\sim_0$ indicates a value at STC conditions. R_S and n are considered constant. Other choices of single diode models are available (e.g., [4]; [5]).

3 METHODS

Parameter estimation for the single diode model determines values for each parameter appearing in Eq. (2) through (5), namely: I_{L0}, α_{Isc}, I_{O0}, E_{g0}, R_{SH0}, R_S, and n.

3.1 Review of Parameter Estimation Methods

The literature describing proposed methods for extracting values for the five parameters appearing in Eq. (1) is extensive; as early as 1986, proposed methods were sufficiently numerous to merit comparative studies (e.g., [6]). Here, we do not attempt a comprehensive literature survey; instead we cite examples that illustrate different approaches to parameter estimation.

Some proposed methods (e.g., [7]; [8]) simplify or replace the diode equation (Eq. (1)) to overcome its implicit nature before extracting parameters. We do not consider these techniques, because fundamentally, they estimate parameters for a different model than Eq. (1).

Techniques that do not simplify the diode equation can be divided roughly into two categories: methods that only use values typically found on a manufacturer's data sheet, i.e., I_{SC}, V_{OC}, etc. (e.g., [9]); and methods that use, in some manner, the full range of measured voltage and current data on the IV curve. In either case, parameter estimation involves solving a system of non-linear equations by numeric methods. Typically, a system of non-linear equations is formulated by evaluating Eq. (1) at specific conditions to obtain equations corresponding to different points on the I-V curve. For example, [3], [5] and [10] evaluate Eq. 1 at STC for the short-circuit, open-circuit and maximum power points, to obtain three equations involving five unknowns; a fourth equation is obtained by setting $dP/dV = 0$ at the maximum power point, and a fifth equation is obtained by translating an I-V curve to a cell temperature different from STC (using temperature coefficients determined by some other method). Other proposed methods obtain a system of equations by making approximations to Eq. (1) over parts of its domain (e.g., [11], [12]) or to equations derived from Eq. (1) (e.g., [13], [14], [15]). The system of equations is then solved by a numerical technique: proposed methods include root-finding (e.g., [16], [5]) and global optimization (e.g., [17], [18]) both of which involve iteration to (i) solve Eq. (1) for current (or voltage), (e.g., [16]) and (ii) adjust parameter values to minimize the error metric.

When formulating the system of equations it is common to adopt the approximation (e.g., [14], [19]):

$$R_{sh} \approx -\left.\frac{dV}{dI}\right|_{I=I_{SC}} \quad (6)$$

Use of this approximation simplifies the system of equations to be solved. However, preliminary work with synthetic IV curves showed that using this approximation and computing the derivative numerically results in erroneous values for R_{sh} by as much as 20%. The source of the error derives from the assumption in Eq. (6) that all terms other than R_{sh} in the exact expression ([20], Eq. 7) for the derivative are negligible, when in fact these terms may amount to a substantial fraction of R_{sh}.

Several methods have been proposed (e.g., [21], [22]) that fit the integrated I-V curve to integrated data by regression; the two cited examples differ in the variable of integration (voltage in the case of [21]; current in the case of [22]). Fitting to integrated data offers the advantage of suppressing the effects of random measurement error but such methods appear to be quite sensitive to systematic measurement or numerical errors.

3.2 Parameter Estimation Methods Considered

We consider three parameter estimation techniques:

1. A method [16] which uses only information typically found on a manufacturer's data sheet, which represents the most commonly-used technique to calibrate the single-diode model;
2. A regression technique [21];
3. A sequential estimation method in development at Sandia National Laboratories [23].

All three methods use a common set of temperature coefficients determined separately from outdoor measurements ([24], [25]). Using these coefficients cell temperature T_C (°C) is calculated from I_{SC} and V_{OC} similar to the method described in IEC 60904-5 [26]. Effective irradiance (W/m^2) (i.e., the irradiance that is converted to electrical current) is estimated from short-circuit current I_{SC}:

$$E = I_{SC}\Big/I_{SC0}\left(1 + \alpha_{Isc}\left(T_C - T_0\right)\right) \times 1000 \text{ W/m}^2 \quad (7)$$

The data sheet method [16] uses short circuit, open circuit and maximum power points on a single IV curve at STC conditions to obtain the STC values (i.e., subscript $\sim_0$ in Eq. (2) through (5)) of each parameter except E_{g0} which is fixed at 1.121eV. In our work, we selected one IV curve measured at conditions close to STC and translated the measurements to STC using IEC 61853-1 [27]. The selected data sheet method is representative of the most commonly-used parameter estimation techniques.

The regression technique [21] estimates a set of five values (i.e., I_L, I_O, R_s, R_{sh}, and n) for each IV curve, then determines model parameters (including E_{g0}) by unweighted regressions against temperature and/or irradiance, as indicated by Eq. (2) through (5).

The sequential method (a preliminary version was reported in [23]) first estimates V_{OC0} (i.e., V_{OC} at STC) and the diode factor n from measured V_{OC} using linear regression as is done for the Sandia Array Performance Model (SAPM; [25]):

$$V_{OC} - \beta_{Voc}\left(T_C - T_0\right) = V_{OC0} + nN_SV_{th}\ln\left(E/E_0\right) \quad (8)$$

where $T_0 = 25°\text{C}$ and β_{Voc} (V/°C) is the previously-determined temperature coefficient of V_{OC}. Eq. (8) can be shown to be asymptotically approximate to Eq. (11) at V_{OC} [28] thus the value obtained for n is appropriate

also for Eq. (1). Next, conditional on this value for n, values for I_L, I_O, R_s, and R_{sh} are determined for each IV curve by an iterative technique [23], and finally model parameters in Eq. (2) through (5) are determined by regression.

3.3 Modules Considered

Single modules of different technologies were mounted on a two-axis tracker located at Sandia National Laboratories in Albuquerque, NM, and IV curves were recorded for a wide range of irradiance and temperature conditions [24]. Table I lists the modules considered and the number of recorded IV curves. Separate testing was conducted with each module to determine temperature coefficients. We retain the nomenclature used in a separate analysis [24], which compares different performance models for these same modules.

Table I: Modules Considered.

Module	STC power	Fill factor	IV curves
Mono-Si-1	305 W	0.77	856
Mono-Si-3	335 W	0.79	1790
Poly-Si-2	230 W	0.73	2973
CdTe-1	70 W	0.62	2951
CIGS-2	225 W	0.73	2597
CIGS-3	225 W	0.65	2934

Note: CIGS-2 and CIGS-3 are preproduction modules

3.4 Numerical technique

Eq. (1) is implicit. However, explicit expressions of $I = I(V)$ (and $V = V(I)$) are obtained by use of the transcendental Lambert's W function (i.e., the solution $W(x)$ of $x = W(x)\exp W(x)$; [29]) as have been published by several authors ([20]; [30]):

$$I = \frac{R_{SH}}{R_{SH}+R_S}(I_L + I_O) - \frac{V}{R_{SH}+R_S} - \frac{nV_{th}}{R_S}W(\theta) \quad (9)$$

$$\theta = \frac{R_S I_O}{nV_{th}}\frac{R_{SH}}{R_{SH}+R_S}\exp\left(\frac{R_{SH}}{R_{SH}+R_S}\frac{R_S(I_L+I_O)+V}{nV_{th}}\right) \quad (10)$$

$$V = (I_L + I_O - I)R_{SH} - IR_S - nV_{th}W(\psi) \quad (11)$$

$$\psi = \frac{I_O R_{SH}}{nV_{th}}\exp\left(\frac{(I_L+I_O-I)R_{SH}}{nV_{th}}\right) \quad (12)$$

Numerically precise algorithms are available to compute values of Lambert's W (e.g., [31]) and we use Eq. (9) and Eq. (10), or Eq. (11) and Eq. (12), to compute solutions of Eq. (1).

4 ANALYSIS

We first investigated convergence of each estimation method by estimating the five values for each measured IV curve, using these five values to calculate each IV curve using only Eq. (1), and comparing the calculated IV curves with measurements. We next found a set of parameter values (i.e., I_{L0}, α_{Isc}, I_{O0}, E_{g0}, R_{SH0}, R_S, and n) for each module, and used the full single diode model (i.e., Eq. (1) through Eq. (5)) to predict IV curves for the irradiance and temperature conditions observed for each measured IV curve. We then compared these predicted IV curves with the measurements to determine how well the fitted model describes each module's performance. Finally, where fitted models diverge from measurements, we examined the structural causes for these model errors.

4.1 Convergence

For the sequential method we found excellent agreement between measured IV curves and points on the IV curves calculated from Eq. (1) using the five parameter values obtained for each IV curve. Figure 1 illustrates convergence of the parameter estimation process for I_{SC}, V_{OC}, V_{MP} and I_{MP} on each measured IV curve for the Mono-Si-1 module; similar convergence is achieved for each of the other modules (Table II). The consistently low values for the metric of convergence indicate that the single diode equation (Eq. (1)) is capable of modeling IV curves for a wide range of irradiance and temperature conditions, and for a wide variety of technologies.

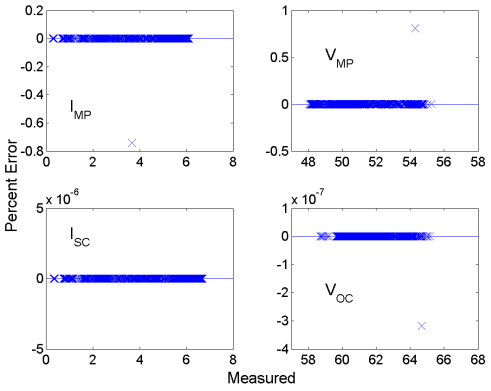

Figure 1: Convergence for each IV curve: sequential method applied to Mono-Si-1 module.

By contrast, the regression method [21] rarely achieved similar convergence (Figure 2). This method uses multiple regression to fit the co-content integral as a 2nd order polynomial in current and voltage over each IV curve, and obtains the five parameter values for an IV curve from non-linear functions which operate on the regression coefficients. Because the predictors are highly collinear over large portions of their ranges, the regression coefficients are quite sensitive to small variations in the data, and frequently, values for n and/or I_O are unreasonably large or small. We found some improvement in performance of this method by first centering and scaling the data using a principal components transform, and by a more careful computation of the co-content integral [28]. However, even after these improvements the resulting values were not reasonable for many IV curves for most modules.

No equivalent analysis of convergence can be done for the data sheet method, which estimates parameters for one IV curve at STC conditions rather than for every IV curve in the data set.

We found that the data sheet method systematically underestimates the diode factor n and the dark current parameter I_{O0} (Table III). Values for n less than 1 are not credible. The underestimation of n likely also causes the underestimated values for I_{O0} because all parameters are determined jointly in the data sheet method. We believe the underestimation for n results from imposing a

fixed value of 1.121 eV for the band gap term E_{g0}. By contrast, the sequential method determines an effective band gap value jointly with I_{O0}, conditional on the value for n determined separately from measured V_{OC} [23]. Values for E_{g0}

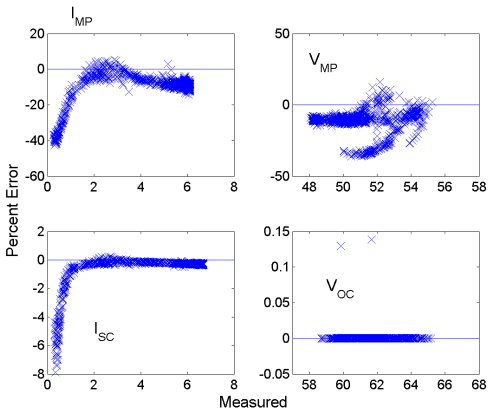

Figure 2: Convergence errors for each IV curve: regression method applied to Mono-Si-1 module.

Table II: Convergence of Sequential Estimation Method.

Module	I_{MP}	V_{MP}	I_{SC}	V_{OC}	RMSE
Mono-Si-1	0.025	0.027	1e-14	1e-8	0.645
Mono-Si-3	0.013	0.013	1e-14	6e-7	0.398
Poly-Si-2	0.010	0.010	1e-14	2e-6	0.574
CdTe-1	0.017	0.018	1e-14	7e-7	0.105
CIGS-2	4e-6	4e-6	1e-14	2e-9	0.433
CIGS-3	2e-4	5e-5	1e-14	3e-5	0.179

Note: Except for RMSE, value is standard deviation of percent error in predicted value. RMSE is 95th percentile of RMSE for each predicted IV curve.

Table III: Comparison of Sequential and Data Sheet Estimation Methods.

	Diode factor n		Dark current I_{O0} (nA)		Band gap E_{g0} (eV)
Module	Seq.	Data sheet	Seq.	Data sheet	Seq.
Mono-Si-1	1.17	1.02	1.06	0.050	0.917
Mono-Si-3	1.11	0.95	0.047	0.0007	0.994
Poly-Si-2	1.05	0.94	1.05	0.15	0.967
CdTe-1	1.48	0.91	0.59	1e-6	0.848
CIGS-2	1.56	0.99	770	0.09	0.684
CIGS-3	1.95	0.94	29,000	0.2	0.537

4.2 Prediction accuracy

We next used the five values for each IV curve to estimate model parameters for Eq. (2) through (5) and then used the full model (Eq. (2) through Eq. (5)) to compute predicted IV curves corresponding to each measured IV curve. We compare points on each predicted IV curve with measurements.

For the regression method, we obtained unreasonable parameter values for all but the Mono-Si-1 module. For example, the regression method estimated a diode factor of 2.96 for the Mono-Si-3 module which is comprised of single junction c-Si cells; for the Poly-Si-2 and all thin film modules, negative values were returned for I_{O0} or E_{g0}, or both. Consequently we show results from the regression method only for the Mono-Si-1 module.

For the sequential and regression methods, parameters in Eq. (3) and Eq. (4) (i.e., I_{O0} and E_{g0}) are estimated jointly in a regression involving estimated I_O values and T_C for each IV curve [23]. We found these fits to be satisfactory for all modules only for the sequential method. Interestingly, we found poor fits when theoretical values for E_{g0} were imposed (e.g., 1.121eV for crystalline silicon modules), indicating that accurate fitting may require regarding E_{g0} as an "effective" band gap for the module as a whole, rather than as a theoretical value at the cell level.

Figure 3 compares errors in model predictions for I_{MP}, V_{MP}, I_{SC} and V_{OC} for the Mono-Si-1 module calculated using Eq. (1) through Eq. (5) with parameters from each estimation method. The regression technique performs worse, with relatively large and biased errors in all four values. The data sheet method performed better but still shows small bias in predicted I_{MP} and I_{SC}. The sequential technique produced parameters for which model prediction have low error (except for I_{MP}) and are generally unbiased. Similar comparisons between the sequential and data sheet methods were observed for the Mono-Si-3 and Poly-Si-1 modules. Table IV compares the estimated parameter values for the Mono-Si-1 module. It is likely that a significant amount of the bias in predicted current for the data sheet method arises from the imposed value for E_{g0}, which causes the value for I_{O0} to be erroneously small.

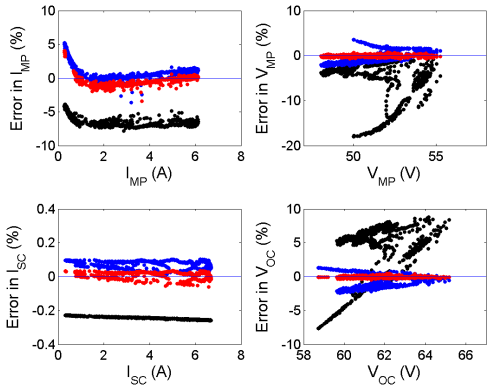

Note: Blue – data sheet; black – regression; red – sequential.

Figure 3: Prediction errors for each IV curve for the Mono-Si-1 module.

Figure 4 compares errors in model predictions for I_{MP}, V_{MP}, I_{SC} and V_{OC} for the CdTe-1 module for the data sheet and sequential methods (the regression method returned negative values for I_{O0} and E_{g0}). The sequential method yields better predictions of voltage but not necessarily of current; predictions show similar systematic errors for both estimation methods. These systematic errors demonstrate that even when fit to well-converged values for each IV curve, the model equations (i.e., Eq. (2) through Eq. (5)) are deficient when applied to the CdTe-1 module. Similar results were found for the other thin-film modules.

Table IV: Estimated parameter values for the Mono-Si-1 module.

	Method		
	Data sheet	Regression	Sequential
I_{L0}	5.968 A	5.946 A	5.964 A
I_{O0}	4.98e-11 A	2.28e-4 A	1.06e-9 A
E_{g0}	1.121 eV (1)	0.467 eV	0.9165 eV
n	1.02	2.81	1.17
R_{SH0}	378 Ω	966 Ω	328 Ω
R_S	0.57 Ω	0.34 Ω	0.48 Ω
α_{Isc}	2.2 mA/C(2)	2.2 mA/C(2)	2.2 mA/C(2)
β_{Voc}	-0.187 V/C(3)	(not used)	-0.187 V/C(3)

(1) assumed value.
(2) common to all methods, estimated from separate measurements.
(3) estimated from separate measurements.

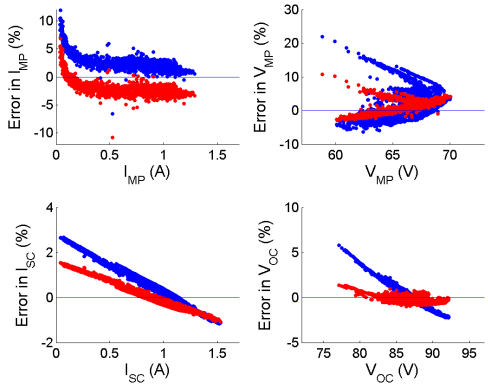

Note: Blue – data sheet; red – sequential.
Figure 4: Prediction errors for each IV curve for the CdTe-1 module.

The sequential method offers the distinct advantage of not only identifying when model equations are deficient, but also yields a data set (i.e., a set of well-calibrated values for each IV curves) which can lead to better equations. For example, the assumption of constant R_S significantly contributes to the errors in predicted I_{MP}. Figure 5 shows estimated and modeled R_S values for the Mono-Si-1 module. If a better fit is made to these estimated values, the prediction errors in I_{MP} (Figure 3) are greatly reduced. However, the equation that improves the R_S model for the Mono-Si-1 module is not general, as is illustrated by Figure 6 for the CdTe-1 module. Plots of R_S vs. irradiance for the other four modules showed a variety of trends.

A similar variety of trends were observed when plotting values for R_{SH} against irradiance (Figure 7 and Figure 8; note the log scale in use.) We found relatively poor agreement between Eq. (5) and the values of R_{SH} for each IV curve, for all modules. We fit Eq. (5) using a robust regression rather than linear regression, and filtered for $E > 400$ W/m^2, because values of R_{SH} can range over several orders of magnitude. The lack of a precise fit arises in part from the relatively large variance in the R_{SH} values, which itself may arise from small

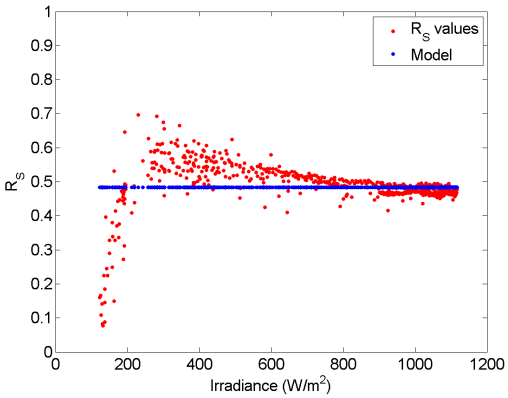

Figure 5: Estimated and modeled values for R_S for each IV curve for the Mono-Si-1 module.

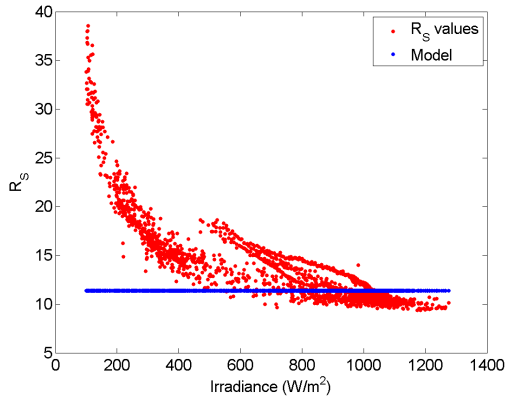

Figure 6: Estimated and modeled values for R_S for each IV curve for the CdTe-1 module.

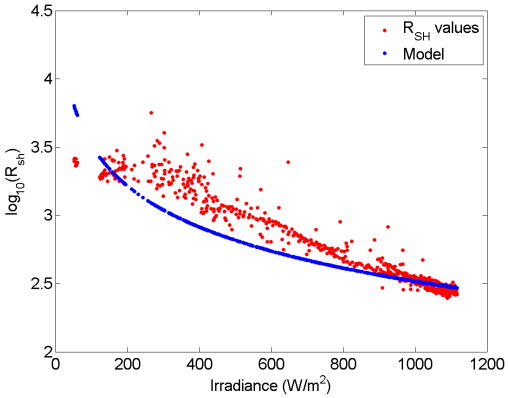

Figure 7: Estimated and modeled values for R_{SH} for each IV curve for the Mono-Si-1 module.

variations in measured current during each IV sweep (because R_{SH} is asymptotically related to the change in current as voltage increases from 0). However, in spite of errors in current measurements, the systematic trends in R_{SH} with effective irradiance is often not well-described by Eq. (5).

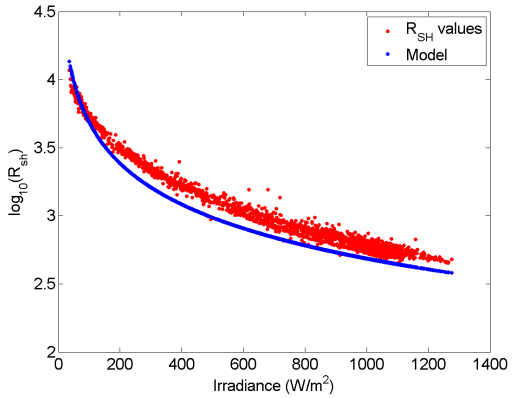

Figure 8: Estimated and modeled values for R_{SH} for each IV curve for the CdTe-1 module.

For all modules, the errors in predicted I_{SC} originate primarily from the regression used to fit Eq. (2). The most significant term in predicted I_{SC} is I_L. To see this, evaluate Eq. (9) at $V=0$, and recognize that $\theta(V=0) \approx \frac{R_S I_O}{nV_{th}} << 1$, so that:

$$I_{SC} = \frac{R_{SH}}{R_{SH}+R_S}(I_L + I_O) - \frac{nV_{th}}{R_S} W\left(\theta(V=0)\right) \approx \frac{R_{SH}}{R_{SH}+R_S}(I_L + I_O) \approx I_L \quad (13)$$

Eq. (2) is fit by a linear regression of I_L for each IV curve onto corresponding measurements of E and T_C. However, the regression often leaves residuals with systematic behavior (Figure 9) which mirror the prediction errors for I_{SC}. Eq. (13) shows a more complex relationship between I_L and I_{SC} which could be the basis for fitting an equation different from Eq. (2) if measurements of both quantities are available. However, we know of no method to directly measure I_L.

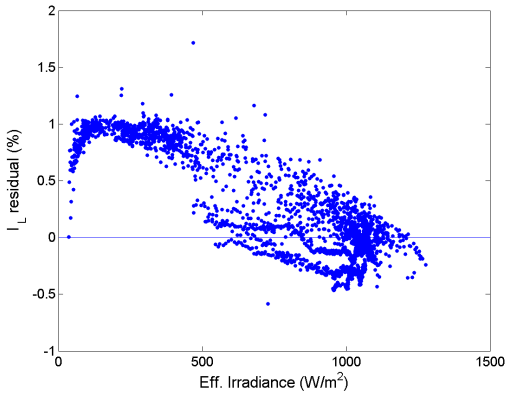

Figure 9: Residuals in the regression for I_L for the CdTe-1 module.

5. CONCLUSION

We have investigated the capability of several parameter estimation methods to produce accurate models of PV modules by calibrating a single diode model to IV curves measured outdoors. We found that the sequential estimation method [23] produced models with smaller prediction errors than result from models calibrated with other methods. By contrast, a regression method [21] was not reliable; and one typically-used data sheet method [16] returned values for several parameters that are not credible. The best-calibrated models produced by the sequential estimation method still showed systematic errors when comparing model predictions to measurements. Because the sequential estimation method is well-converged to each measured IV curve, the model prediction errors result from deficiencies in the model equations themselves, rather than from poorly chosen parameters. To improve the single diode model, the IV-curve-specific values can be used to formulate new model equations which will improve model accuracy.

6. ACKNOWLEGEMENTS

Sandia is a multiprogram laboratory operated by Sandia Corporation, a Lockheed Martin Company, for the United States Department of Energy's National Nuclear Security Administration under contract DE-AC04-94AL85000.

7. REFERENCES

[1] J.L. Gray, The Physics of the Solar Cell, in: A. Luque, Hegedus, S. (Ed.) Handbook of Photovoltaic Science and Engineering, John Wiley and Sons, 2011.
[2] A. Mermoud, T. Lejeune, Performance Assessment Of A Simulation Model For Pv Modules Of Any Available Technology, in: 25th European Photovoltaic Solar Energy Conference, Valencia, Spain, 2010.
[3] W. De Soto, S.A. Klein, W.A. Beckman, Improvement and validation of a model for photovoltaic array performance, Solar Energy, 80 (2006) 78-88.
[4] User's Guide PVsyst Contextual Help, http://files.pvsyst.com/pvsyst5.pdf, 2010.
[5] H. Tian, F. Mancilla-David, K. Ellis, E. Muljadi, P. Jenkins, A cell-to-module-to-array detailed model for photovoltaic panels, Solar Energy, 86 (2012) 2695-2706.
[6] D.S.H. Chan, J.C.H. Phang, Analytical methods for the extraction of solar-cell single- and double-diode model parameters from I-V characteristics, Electron Devices, IEEE Transactions on, 34 (1987) 286-293.
[7] S. Karmalkar, S. Haneefa, A Physically Based Explicit Model of a Solar Cell for Simple Design Calculations, Electron Device Letters, IEEE, 29 (2008) 449-451.
[8] F. Bonanno, G. Capizzi, G. Graditi, C. Napoli, G.M. Tina, A radial basis function neural network based approach for the electrical characteristics estimation of a photovoltaic module, Applied Energy, 97 (2012) 956-961.
[9] G. Farivar, B. Asaei, Photovoltaic module single diode model parameters extraction based on manufacturer datasheet parameters, in: Power and Energy (PECon), 2010 IEEE International Conference on, 2010, pp. 929-934.
[10] J.A. Duffie, W.A. Beckman, Solar Engineering of Thermal Processes Wiley, 2006.

[11] W. Kim, W. Choi, A novel parameter extraction method for the one-diode solar cell model, Solar Energy, 84 (2010) 1008-1019.
[12] J.C.H. Phang, D.S.H. Chan, J.R. Phillips, Accurate analytical method for the extraction of solar cell model parameters, Electronics Letters, 20 (1984) 406-408.
[13] E. Dallago, D. Finarelli, P. Merhej, Method based on single variable to evaluate all parameters of solar cells, Electronics Letters, 46 (2010) 1022-1024.
[14] K.I. Ishibashi, Y. Kimura, M. Niwano, An extensively valid and stable method for derivation of all parameters of a solar cell from a single current-voltage characteristic, J. Appl. Phys., 103 (2008).
[15] S.K. Datta, K. Mukhopadhyay, S. Bandopadhyay, H. Saha, An improved technique for the determination of solar cell parameters, Solid State Electron, 35 (1992) 1667-1673.
[16] A.P. Dobos, An Improved Coefficient Calculator for the California Energy Commission 6 Parameter Photovoltaic Module Model, Journal of Solar Energy Engineering, 134 (2012).
[17] K.M. El-Naggar, M.R. AlRashidi, M.F. AlHajri, A.K. Al-Othman, Simulated Annealing algorithm for photovoltaic parameters identification, Solar Energy, 86 (2012) 266-274.
[18] E.Q.B. Macabebe, C.J. Sheppard, E.E. van Dyk, Parameter extraction from I–V characteristics of PV devices, Solar Energy, 85 (2011) 12-18.
[19] M. Chegaar, G. Azzouzi, P. Mialhe, Simple parameter extraction method for illuminated solar cells, Solid State Electron, 50 (2006) 1234-1237.
[20] A. Jain, A. Kapoor, Exact analytical solutions of the parameters of real solar cells using Lambert W-function, Solar Energy Materials and Solar Cells, 81 (2004) 269-277.
[21] A. Ortiz-Conde, F.J. García Sánchez, J. Muci, New method to extract the model parameters of solar cells from the explicit analytic solutions of their illuminated I–V characteristics, Solar Energy Materials and Solar Cells, 90 (2006) 352-361.
[22] L. Peng, Y. Sun, Z. Meng, Y. Wang, Y. Xu, A new method for determining the characteristics of solar cells, Journal of Power Sources, 227 (2013) 131-136.
[23] C. Hansen, Estimation of Parameters for Single Diode Models Using Measured IV Curves, in: 39th IEEE Photovoltaic Specialists Conference, Tampa, FL, 2013.
[24] J.S. Stein, Sutterlueti, J., Ransome, S., Hansen, C. W., King, B. H., Outdoor PV Performance Evaluation of Three Different Models: Single-Diode, SAPM and Loss Factor Model, in: 28th European PV Solar Energy Conference, Paris, France, 2013.
[25] C. Hansen, J. Stein, S. Miller, E.E. Boyson, J.A. Kratochvill, D.L. King, Parameter Uncertainty in the Sandia Array Performance Model for Flat-Plate Crystalline Silicon Modules, in: IEEE Photovoltaics Specialists Conference, Seattle, WA, 2011.
[26] I.E.C. (IEC), 60904-5 Ed. 2.0: Photovoltaic devices - Part 5: Determination of the equivalent cell temperature (ECT) of photovoltaic (PV) devices by the open-circuit voltage method, 2011.
[27] I.E.C. (IEC), 61853-1 Ed. 1.0: Photovoltaic (PV) module performance testing and energy rating - Part I: Irradiance and temperature performance measurements and power rating, 2011.
[28] C. Hansen, Parameter Estimation for Single Diode Models of Photovoltaic Modules, in, Sandia National Laboratories, Albuquerque, NM, Forthcoming.
[29] R.M. Corless, G.H. Gonnet, D.E.G. Hare, D.J. Jeffrey, D.E. Knuth, On the Lambert W Function in: Advances in Computational Mathematics, 1996, pp. 329-359.
[30] A. Ortiz-Conde, F.J. García Sánchez, J. Muci, Exact analytical solutions of the forward non-ideal diode equation with series and shunt parasitic resistances, Solid State Electron, 44 (2000) 1861-1864.
[31] D.A. Barry, S.J. Barry, P.J. Culligan-Hensley, Algorithm-743 - Wapr - a Fortran Routine for Calculating Real Values of the W-Function, Acm T Math Software, 21 (1995) 172-181.